SQSTM1 splice site mutation in distal myopathy with rimmed vacuoles

Robert C. Bucelli, MD, PhD*
Khalid Arhzaouy, PhD*
Alan Pestronk, MD
Sara K. Pittman, BS
Luisa Rojas, MD
Carolyn M. Sue, MBBS, PhD
Anni Evilä, BS
Peter Hackman, PhD
Bjarne Udd, MD, PhD
Matthew B. Harms, MD
Conrad C. Weihl, MD, PhD

Correspondence to Dr. Weihl: weihlc@neuro.wustl.edu

ABSTRACT

Objective: To identify the genetic etiology and characterize the clinicopathologic features of a novel distal myopathy.

Methods: We performed whole-exome sequencing on a family with an autosomal dominant distal myopathy and targeted exome sequencing in 1 patient with sporadic distal myopathy, both with rimmed vacuolar pathology. We also evaluated the pathogenicity of identified mutations using immunohistochemistry, Western blot analysis, and expression studies.

Results: Sequencing identified a likely pathogenic c.1165+1 G>A splice donor variant in *SQSTM1* in the affected members of 1 family and in an unrelated patient with sporadic distal myopathy. Affected patients had late-onset distal lower extremity weakness, myopathic features on EMG, and muscle pathology demonstrating rimmed vacuoles with both TAR DNA-binding protein 43 and SQSTM1 inclusions. The c.1165+1 G>A *SQSTM1* variant results in the expression of 2 alternatively spliced SQSTM1 proteins: 1 lacking the C-terminal PEST2 domain and another lacking the C-terminal ubiquitin-associated (UBA) domain, both of which have distinct patterns of cellular and skeletal muscle localization.

Conclusions: SQSTM1 is an autophagic adaptor that shuttles aggregated and ubiquitinated proteins to the autophagosome for degradation via its C-terminal UBA domain. Similar to mutations in *VCP,* dominantly inherited mutations in *SQSTM1* are now associated with rimmed vacuolar myopathy, Paget disease of bone, amyotrophic lateral sclerosis, and frontotemporal dementia. Our data further suggest a pathogenic connection between the disparate phenotypes. ***Neurology*®** **2015;85:665–674**

GLOSSARY

AD = autosomal dominant; **ALP** = alkaline phosphatase; **ALS** = amyotrophic lateral sclerosis; **cDNA** = complementary DNA; **CK** = creatine kinase; **EDL** = extensor digitorum longus; **EM** = electron microscopy; **FDI** = first dorsal interosseous; **FTD** = frontotemporal dementia; **gDNA** = genomic DNA; **IBM** = inclusion body myopathy; **LC3** = microtubule-associated protein 1A light chain-3; **MSP** = multisystem proteinopathy; **NCS** = nerve conduction studies; **PBS** = phosphate-buffered saline; **PDB** = Paget disease of bone; **RV** = rimmed vacuole; **TA** = tibialis anterior; **TDP-43** = TAR DNA-binding protein 43; **UBA** = ubiquitin-associated.

Distal myopathies are a heterogeneous group of muscle diseases inherited in an autosomal dominant (AD) or autosomal recessive manner.[1] More than 20 different genetic causes of distal myopathy have been described.[1] One subset of distal myopathies is characterized as late onset with AD inheritance. Many of these myopathies have vacuolation or myofibrillar disorganization on muscle biopsy.

Mutations in proteins typically associated with other muscle phenotypes, such as limb-girdle or scapuloperoneal weakness, can also lead to a distal myopathy. For example, mutations in *DES* cause limb-girdle, scapuloperoneal, or distal weakness.[2] Similarly, mutations in *VCP* that cause inclusion body myopathy (IBM) associated with Paget disease of bone (PDB), frontotemporal dementia (FTD), and amyotrophic lateral sclerosis (ALS) have been reported to cause a limb-girdle myopathy, scapuloperoneal dystrophy, and a distal myopathy.[3,4] Similar to other distal

Editorial, page 658

*These authors contributed equally to the manuscript.

From the Department of Neurology (R.C.B., K.A., A.P., S.K.P., M.B.H., C.C.W.), Washington University School of Medicine, Saint Louis, MO; Dent Neurologic Institute (L.R.), Amherst, NY; Department of Neurogenetics (C.M.S.), Kolling Institute of Medical Research, Royal North Shore Hospital and University of Sydney, St Leonard's, New South Wales, Australia; Folkhalsan Institute of Genetics and Department of Medical Genetics (A.E., P.H., B.U.), Haartman Institute, University of Helsinki, Finland; Neuromuscular Research Center (B.U.), Tampere University Hospital and University of Tampere, Finland; and Department of Neurology (B.U.), Vaasa Central Hospital, Vaasa, Finland.

Go to Neurology.org for full disclosures. Funding information and disclosures deemed relevant by the authors, if any, are provided at the end of the article.

myopathies, *VCP* myopathy has rimmed vacuoles (RVs) and aggregates of proteins such as SQSTM1 and TAR DNA-binding protein 43 (TDP-43).[5,6] Mutations in *SQSTM1* and *TARDP* are associated with ALS, leading to speculation about a genetic and pathogenic overlap between rimmed vacuolar myopathies and ALS.[7,8] This is further supported by the identification of mutations in *HNRNPA2B1* and *HNRNPA1* as causing varied phenotypic penetrance of IBM and ALS.[9] Whether mutations in other genes can similarly lead to phenotypes consisting of muscle, bone, and CNS dysfunction is not established.

METHODS

Patient selection and evaluation. Patients with muscle weakness of unknown genetic cause were identified from the Washington University Neuromuscular Genetics Project and from the international cohort of undetermined distal myopathies at the Neuromuscular Research Center in Finland. Charts, clinical records, and pathology were reviewed, and available individuals were reexamined.

Standard protocol approvals, registrations, and patient consents. All participants gave written informed consent, and study procedures were approved by the Human Studies Committee at Washington University and the Institutional Review Board of the Helsinki University Hospital.

Histochemistry and immunohistochemistry. Muscle tissue was processed as previously described.[10] Cryostat sections of frozen muscle were processed and fixed in acetone. Antibodies used were anti-TDP-43 (Proteintech, Chicago, IL) and anti-SQSTM1 (Sigma-Aldrich, St. Louis, MO) for immunohistochemistry, anti-SQSTM1 (Proteintech) for immunoblot, and anti-ubiquitin (Enzo Life Sciences BML-PW8810, Farmingdale, NY), anti-actin rabbit polyclonal antibody (Sigma-Aldrich), mouse anti-ubiquitin FK2 (Enzo Life Sciences BML-PW8810), rabbit anti-mCherry (Rockland Immunochemicals, Inc. 600-401-P16S, Pottstown, PA), rabbit anti-GAPDH antibody (Cell Signaling Technology 2118, Danvers, MA), and LC3 (NanoTools, Teningen, Germany). U2OS cells were cultured on coverslips and transfected using Lipofectamine 2000 (Invitrogen, Waltham, MA). Transfected cells were washed with phosphate-buffered saline (PBS) and fixed in 3.7% paraformaldehyde for 10 minutes, washed in PTB (1x PBS, 0.1% Triton X-100, 0.1% bovine serum albumin), incubated in primary antibodies at a 1:100 dilution at 4°C overnight, and washed with PTB buffer. Cells were incubated with Alexa Fluor 488 goat anti-mouse secondary antibody (Invitrogen) at a 1:1,000 dilution and washed as above. Coverslips were mounted on slides using Mowiol reagent containing 4',6-diamidino-2-phenylindole (1:1,000). Images were acquired with a CoolSNAP EZ camera on a Nikon Eclipse 80i microscope with NIS-Elements AR 3.00 software (Nikon, Tokyo, Japan). Mouse tibialis anterior (TA) electroporation and visualization were performed as previously described.[5]

Electron microscopy. Muscle was fixed in modified Karnovsky fixative and processed as previously described.[5] Slides were viewed with a JEOL model 1200EX electron microscope (JEOL, Tokyo, Japan). Images were acquired using the AMT Advantage HR high-definition CCD, 1.3 megapixel transmission electron microscopy camera (Advanced Microscopy Techniques, Woburn, MA).

Whole-exome sequencing and targeted exome sequencing. Indexed genomic DNA (gDNA) libraries were prepared from gDNA using TruSeq DNA Preparation Kit (Illumina, San Diego, CA) and exome capture using TruSeq Exome Enrichment Kit (Illumina), according to the manufacturer's protocol. Sequencing was performed with 100 bp paired-end reads on a HiSeq2000 (Illumina). For targeted sequencing, gDNA was captured using SeqCap EZ Choice Library (Roche NimbleGen, Madison, WI), which was designed to target exons of 180 myopathy-related genes. Sequencing was performed with 100 bp paired-end reads on a HiSeq1500 (Illumina) at the Institute for Molecular Medicine Finland. Reads were aligned to the human reference genome with NovoAlign or Burrows-Wheeler Aligner. Variants were called with SAMtools and annotated with SeattleSeq. Coverage across genomic intervals was calculated using BEDTools. Genomic coordinates for regions targeted by the whole-exome capture kit were provided by Illumina. Validation of mutations was assessed with standard PCR-based sequencing using Primer3Plus (http://www.bioinformatics.nl/cgi-bin/primer3plus/primer3plus.cgi) for primer design, an Applied Biosystems 3730 DNA Sequencer (Life Technologies, Carlsbad, CA) for sequencing, and LaserGene SeqMan Pro version 8.0.2 (DNAStar, Madison, WI) for tracing analysis.

Primary fibroblast culture. Fibroblasts were cultured in Fibroblast Basal Medium FGM-2 CC-313 (Lonza, Basel, Switzerland) supplemented with CC-4126, as recommended by the manufacturer, at 37°C and 5% CO_2 in a humidified incubator.

RNA analysis. RNA was isolated from fibroblasts and muscle tissue using SV Total RNA Isolation Kit Z3100 (Promega, Madison, WI). Complementary DNA (cDNA) was prepared by reverse transcription PCR using Transcriptor First Strand cDNA Synthesis Kit from Roche (Basel, Switzerland), according to the manufacturer's instructions. cDNA was PCR amplified with primers specific for exon 7 and exon 9 of *SQSTM1* using the following primers: forward primer 5′-CAGCACAGAGGAGAAGAGCA-3′ and reverse primer 5′-GGGGATGCTTTGAATACTGG-3′. PCR products were analyzed by electrophoresis, purified using QIAquick Gel Extraction Kit 28704 (Qiagen, Venlo, the Netherlands) and cloned into pGEM-T Easy Vector System (Promega). Colonies were sequenced with T7 Forward and SP6 Reverse primers.

Protein analysis. Muscle and fibroblasts were homogenized in radioimmunoprecipitation assay lysis buffer (50 mm Tris–HCl, pH 7.4, 150 mm NaCl, 1% NP-40, 0.25% Na-deoxycholate, and 1 mm ethylenediaminetetraacetic acid) supplemented with protease inhibitor cocktail (Sigma-Aldrich). Lysates were centrifuged at 14,000*g* for 10 minutes. Aliquots were solubilized in Laemmli sample buffer and equal amounts were separated on 10% sodium dodecyl sulfate polyacrylamide gel electrophoresis gels, transferred to nitrocellulose, and blocked with 5% nonfat dry milk in TBS-Tween. Membrane was incubated with antibody at 1:1,000 dilution overnight followed by incubation with secondary antibody conjugated with horseradish peroxidase at a 1:5,000 dilution. Amersham ECL Western Blotting Detection Reagents Kit (GE Healthcare, Chalfont St Giles, UK) was used for protein detection and immunoblots were visualized with G:Box Chemi XT4, Genesys version 1.1.2.0 (Syngene, Cambridge, UK).

RESULTS

Genetic findings. Whole-exome sequencing was performed on the proband of family 1 (figure 1A)

Figure 1 ***SQSTM1*** **variant in 2 unrelated patients with distal myopathy**

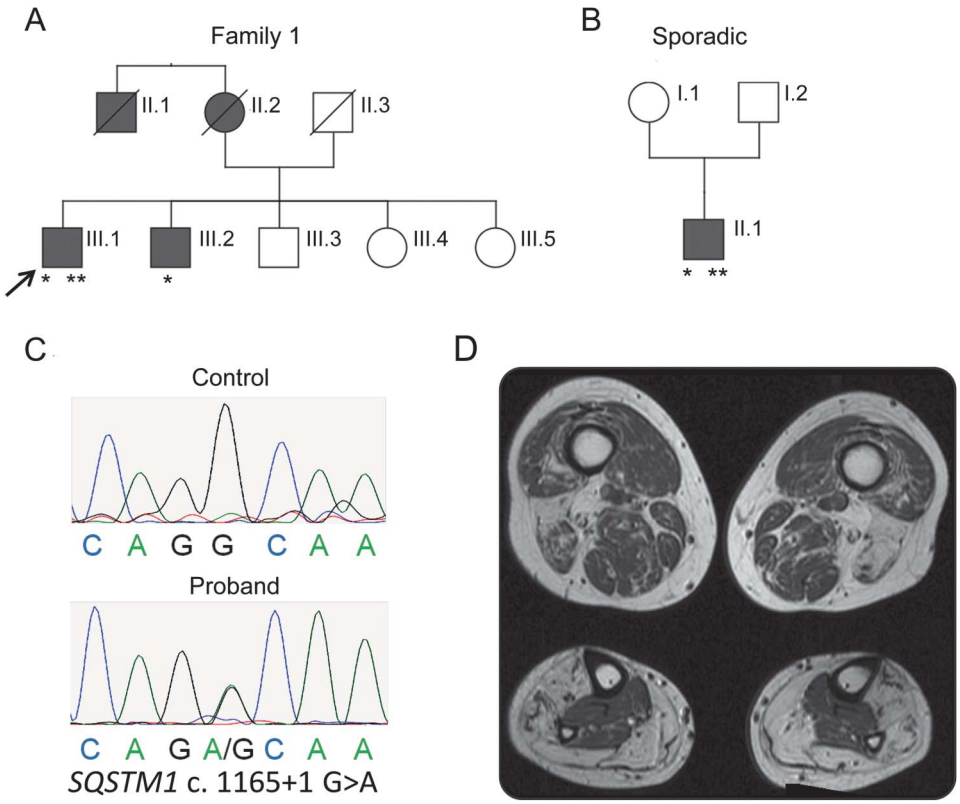

Pedigrees of family 1 (A) and a sporadic patient (B) are shown. Affected patients are in gray and an arrow denotes the proband. *Indicates patients clinically examined and variant carriers, **Indicates patients with muscle biopsies. (C) Representative chromatogram of the forward sequencing reaction in a control and in the proband of family 1. (D) T1-weighted MRI of the thighs (upper images) and calves (lower images) of the patient with sporadic distal myopathy. Note marked atrophy of the biceps femoris with relative sparing of adductors and vastus lateralis and marked atrophy of the soleus, medial gastrocnemius, and tibialis anterior with relative sparing of the extensor hallucis and digitalis longus, tibialis posterior, flexor hallucis, and digitorum longus.

and targeted exome sequencing was performed on an unrelated patient with sporadic distal myopathy (figure 1B). No pathogenic variants in any gene associated with neuromuscular disease were identified. However, a heterozygous c.1165+1 G>A variant in *SQSTM1* was present in both unrelated patients (figure 1C). This variant has a minor allele frequency of 0% in the Single Nucleotide Polymorphism database and the Exome Variant Server and has been previously reported in 2 families with AD PDB[11,12] and in another single patient with sporadic ALS and PDB.[13] Sanger sequencing validated this variant in both patients and in the affected brother from family 1. No DNA was available from either patient's deceased parents.

Patient characteristics. ***Family 1.*** The proband, a 63-year-old man from the United States, developed right ankle dorsiflexion weakness at age 52 and left ankle dorsiflexion weakness at age 57. At age 60 he noted left-greater-than-right "shoulder" weakness resulting in a referral to our institution. Past medical history included right hemidiaphragmatic paralysis, sequential bilateral cranial nerve VII palsies (right: age 38 with complete recovery; left: age 41 with residual weakness), and hypothyroidism. Family history (figure 1A) included his mother, who developed bilateral foot drop in her mid-60s and died at age 83, a similarly affected maternal uncle, and a brother with a similar phenotype (described below). His examination was notable for stigmata of a chronic left facial neuropathy, mild shoulder abduction weakness (left greater than right), bilateral scapular winging, left wrist extensor weakness, and bilateral ankle dorsiflexion and toe extension paresis with moderate plantar flexion weakness and severe toe flexion weakness. Ankle reflexes were absent with negative Babinski signs and a steppage gait. Creatine kinase (CK) was 419 U/L (normal 30–200 U/L) and alkaline phosphatase (ALP) was 87 U/L (normal 37–126 U/L). Nerve conduction studies (NCS) were normal. EMG showed a myopathy with myopathic features in the left extensor digitorum communis, first dorsal interosseous (FDI), abductor pollicis brevis, and right TA and medial gastrocnemius muscles. A radionuclide scan and plain film skeletal survey failed

to identify any Pagetoid lesions. Transthoracic echocardiogram was normal. Forced vital capacity was 60% of predicted. Chromosome 4q35 deletion analysis for facioscapulohumeral dystrophy was negative.

The proband's brother, now 47 years old, developed right ankle dorsiflexion weakness at age 42. At age 45 he had difficulty raising his right arm over his head and sought medical attention. His past medical history is notable for hypothyroidism and hypertension. On examination he had mild bilateral upper facial weakness. He had no scapular winging but did have inverted anterior axillary folds with mild bilateral pectoralis weakness. He had mild bilateral shoulder abduction and wrist extensor weakness, moderate ankle dorsiflexion weakness (right greater than left), and bilateral toe extensor weakness. Reflexes were normal with negative Babinski signs. Sensation and gait were unremarkable. CK was 143 U/L and ALP was 70 U/L. NCS were normal and EMG showed myopathic features in the left flexor pollicus longus and FDI muscles and the right extensor digitorum longus (EDL) and TA muscles. The right TA, EDL, and gastrocnemius also showed fibrillations and positive sharp waves, myotonic discharges, and complex repetitive discharges.

Patient with sporadic distal myopathy. The patient is a 60-year-old man from Australia with progressive distal lower extremity weakness. His symptoms began at age 50 when he developed a bilateral foot drop that progressed over the last 10 years to include finger extensor weakness and atrophy of his medial gastrocnemius muscles and shoulder girdle. He has no family history of muscle weakness, dementia, or PDB. On examination he had asymmetric scapular winging (left greater than right) and asymmetric shoulder weakness (right greater than left), mild hip flexor weakness, and marked weakness of bilateral ankle dorsiflexion and ankle eversion. CK was 346 U/L. He had no complaints of bone pain and his ALP was normal. NCS were normal and EMG was myopathic in his distal muscles. An MRI of his lower extremities demonstrated atrophy of his biceps femoris, soleus, medial gastrocnemius, and TA (figure 1D).

Muscle biopsy. ***Patient III.1.*** A right deltoid biopsy demonstrated marked variation in fiber size, with groups of rounded fibers, many fibers with internal nuclei, and occasional pyknotic nuclear clumps (figure 2A). There was no fiber type grouping on myosin ATPase stains. Several fibers contained RVs (figure 2B). Nicotinamide adenine dinucleotide demonstrated abnormal internal architecture and lobulation in occasional fibers (figure 2C). Immunohistochemistry was notable for scattered fibers containing SMI-31, TDP-43, microtubule-associated protein 1A light chain-3 (LC3), and SQSTM1 positivity (figure 2, D–F). Electron microscopy (EM) demonstrated large foci of myofibrillar disorganization and Z-band streaming (figure 2, G and H).

Sporadic patient. Biopsy was remarkable for variation in fiber size, internal nuclei with fiber splitting, and scattered pyknotic nuclei. Occasional fibers were lobulated and scattered fibers contained multiple RVs. EM was consistent with a dystrophic process and myofibrillar disarray.

Splicing validation and protein studies. The c.1165+1 G>A variant in *SQSTM1* alters a splice donor site at the exon–intron junction of exon 7 and is predicted to disrupt splicing of exon 7 to exon 8. We isolated cDNA from fibroblasts of a control and patient III.1 and PCR amplified exon 6 to exon 9 of *SQSTM1.* The amplified product from the control's fibroblasts migrated as a single band, consistent with intact exon 7–8 splicing (figure 3A). Patient III.1's amplified PCR product migrated as 3 bands: 1 matching the normally spliced messenger RNA and 2 others consistent with alternative splicing due to the utilization of cryptic splice acceptor sites (figure 3A). These PCR products were subcloned and sequenced to identify the cryptic splicing. In addition to the full-length SQSTM1 protein, 2 cryptically spliced SQSTM1 variants were identified in patient III.1's fibroblasts: a SQSTM1 deletion mutation p.G351_P388del (SQSTM1ΔPEST2) that utilized a cryptic splice acceptor within exon 7 and a SQSTM1 truncation mutation p.Glu389delinsAspLysTer (SQSTM1ΔUBA-DK) that utilized a cryptic splice acceptor within intron 7 (figure 3, B and E). These transcripts were also identified in patient III.1's muscle tissue (not shown). To confirm that the truncated and/or deleted SQSTM1 proteins were translated, we immunoblotted for SQSTM1 in fibroblasts from a control and patient III.1. As expected, full-length SQSTM1 was present in control lysates, but patient III.1's lysates contained the full-length protein and a smaller SQSTM1 species migrating at the molecular weight of the predicted deletion and truncating mutants (figure 3C, lower blot). There was also an increase in high-molecular-weight ubiquitin conjugates in patient fibroblasts compared with control fibroblasts (figure 3C, upper blot). Similar to patient fibroblasts, lysate from patient III.1's skeletal muscle showed a decrease in full-length SQSTM1 and the appearance of truncated SQSTM1 species (SQSTM1Δ) (figure 3D). The molecular weight of SQSTM1Δ in patient tissue was consistent with the predicted sizes of the 2 truncated SQSTM1 proteins that migrate similarly on immunoblot (figure 3, E and F).

The cellular localization of full-length SQSTM1, SQSTM1ΔUBA-DK, or SQSTM1ΔPEST2 fused to an N-terminal mCherry protein was assessed in

Figure 2 Muscle histochemistry and immunohistochemistry of *SQSTM1*-associated distal myopathy with rimmed vacuoles

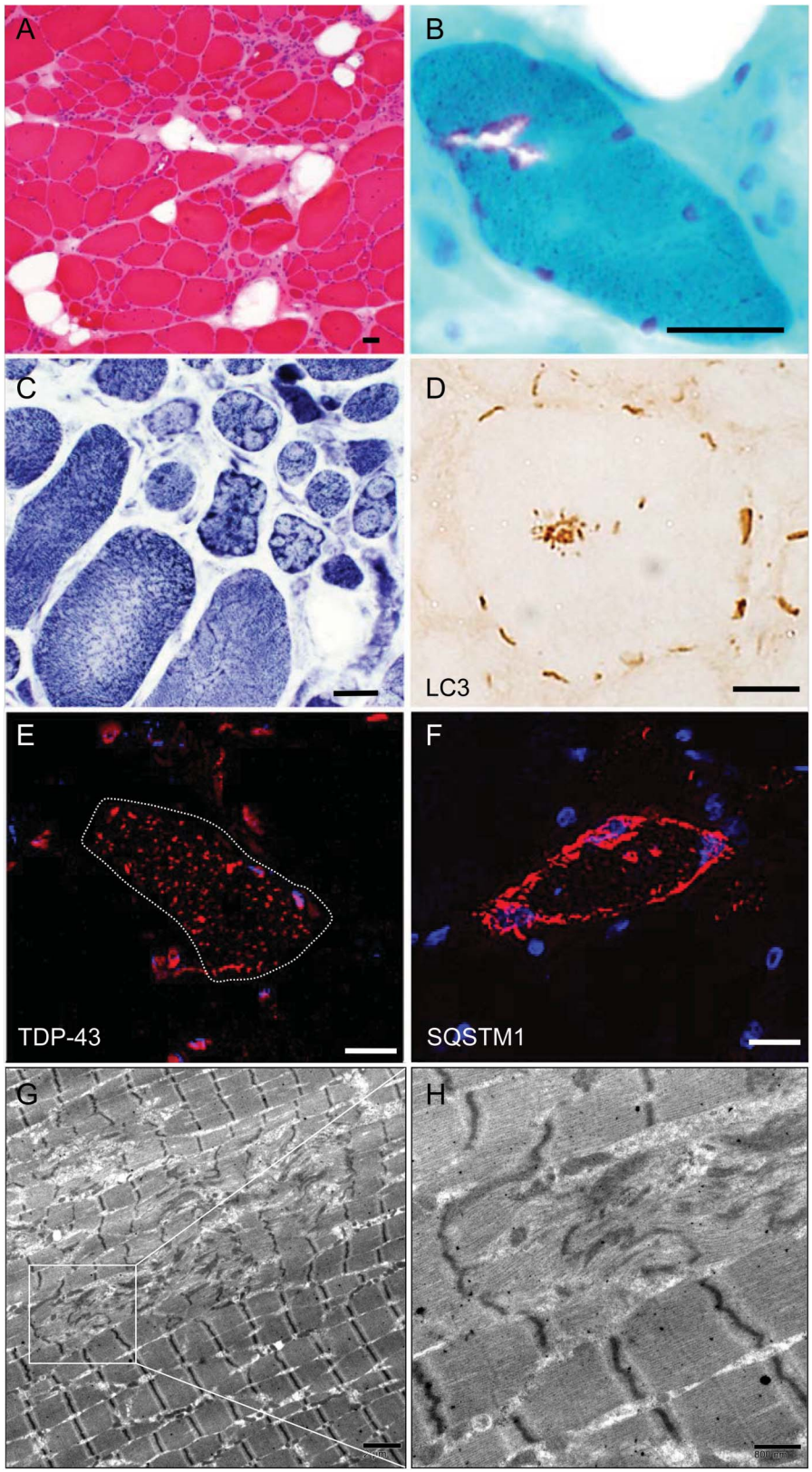

Muscle biopsy of patient III.1 demonstrates a rimmed vacuolar myopathy with lobulated fibers. (A) Hematoxylin and eosin, (B) modified Gomori trichrome staining of a vacuolated fiber, (C) nicotinamide adenine dinucleotide staining showing lobulated fibers. Immunohistochemical staining for (D) microtubule-associated protein 1A light chain-3 (LC3), (E) TAR DNA-binding protein 43 (TDP-43), and (F) SQSTM1. 4′,6-Diamidino-2-phenylindole–stained nuclei are in blue. Scale bar is 15 μm. Electron micrograph of skeletal muscle from patient III.1 demonstrating (G) large focal areas of myofibrillar disorganization and (H) Z-band streaming. Scale bar is 500 nm.

Figure 3 Cryptic splicing of *SQSTM1* in a patient with distal myopathy

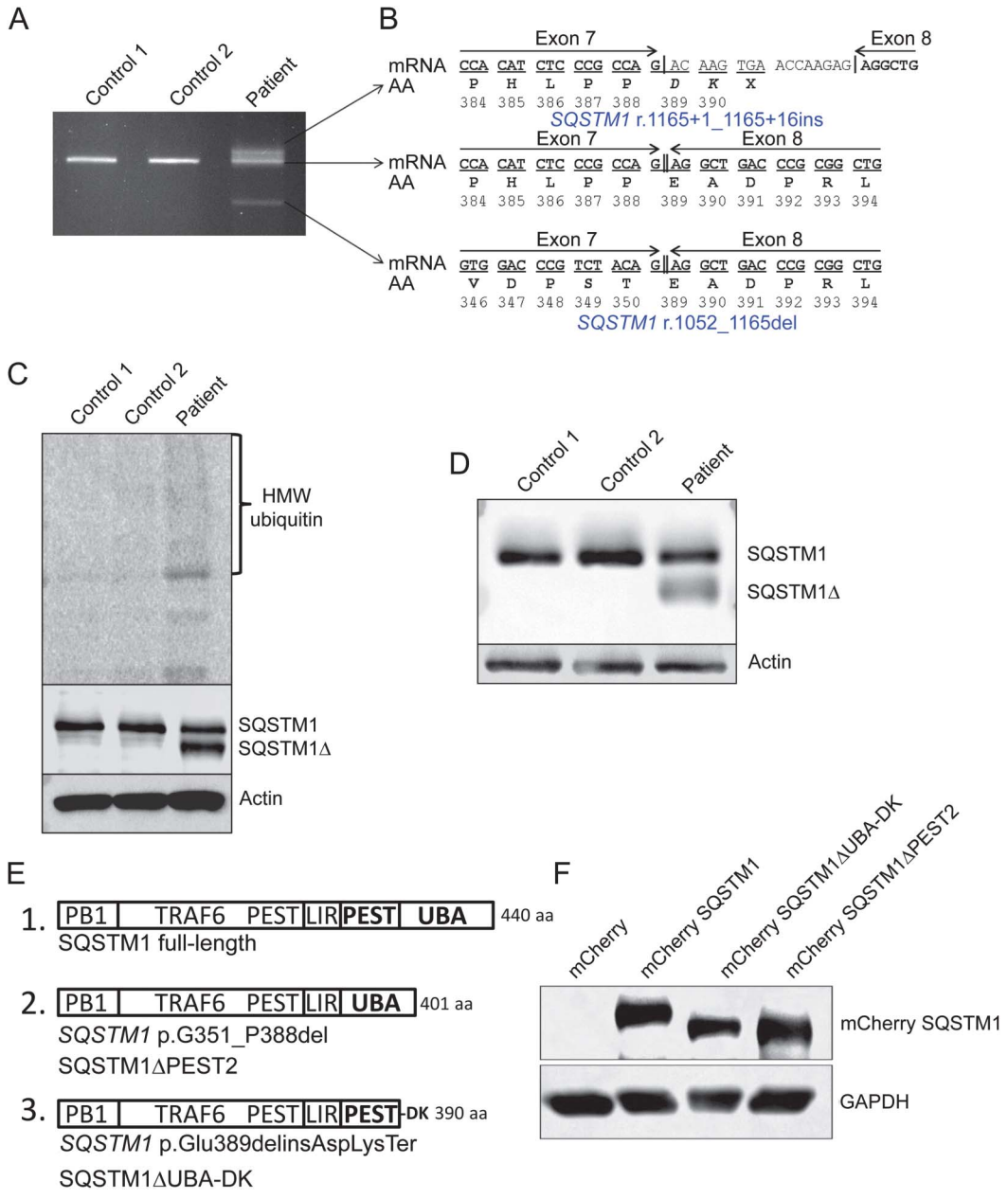

(A) Complementary DNA was isolated from primary fibroblasts of controls or patient III.1 from family 1 and was PCR amplified with primers spanning exon 6 to exon 9 of *SQSTM1*. In contrast to control fibroblasts, patient fibroblasts contain 3 *SQSTM1* transcripts. (B) The sequence of *SQSTM1* transcripts was identified by subcloning each PCR product into pGEM-T easy vector followed by Sanger sequencing. The sequence and resultant translated product are written below each transcript. (C) Lysates from fibroblasts of controls or patient III.1 were immunoblotted with antibodies to SQSTM1, ubiquitin, and actin. Note an increase in high-molecular-weight (HMW) ubiquitinated proteins in patient lysates and the presence of a truncated SQSTM1 protein (SQSTM1Δ). (D) Skeletal muscle lysates from controls or patient III.1 were immunoblotted with an anti-SQSTM1 antibody or actin as a loading control. Note that the patient has a reduction in full-length SQSTM1 and the appearance of a lower molecular weight product, SQSTM1Δ. (E) Diagrams of the 3 putative protein products generated in the patient's muscle: (1) is full-length SQSTM1, (2) lacks amino acids 351–388, which encode the second PEST domain (SQSTM1ΔPEST2), and (3) deletes the C-terminal ubiquitin-associated (UBA) domain with the addition of a C-terminal Asp and Lys (SQSTM1ΔUBA-DK). (F) Immunoblot for SQSTM1 or glyceraldehyde-3-phosphate dehydrogenase (GAPDH) from lysates of U2OS cells transiently transfected with plasmids expressing mCherry alone or mCherry fused to SQSTM1, SQSTM1ΔUBA-DK, or SQSTM1ΔPEST2.

U2OS cells. mCherry was present throughout cells, whereas SQSTM1 was present as small inclusions throughout the cytoplasm that colocalized with LC3 (figure 4A) and ubiquitin (figure 4B). The SQSTM1 deletion mutations had distinct patterns of expression. SQSTM1ΔUBA-DK was present

Figure 4 Cryptically spliced mutant SQSTM1 proteins have distinct cellular and myofiber localization

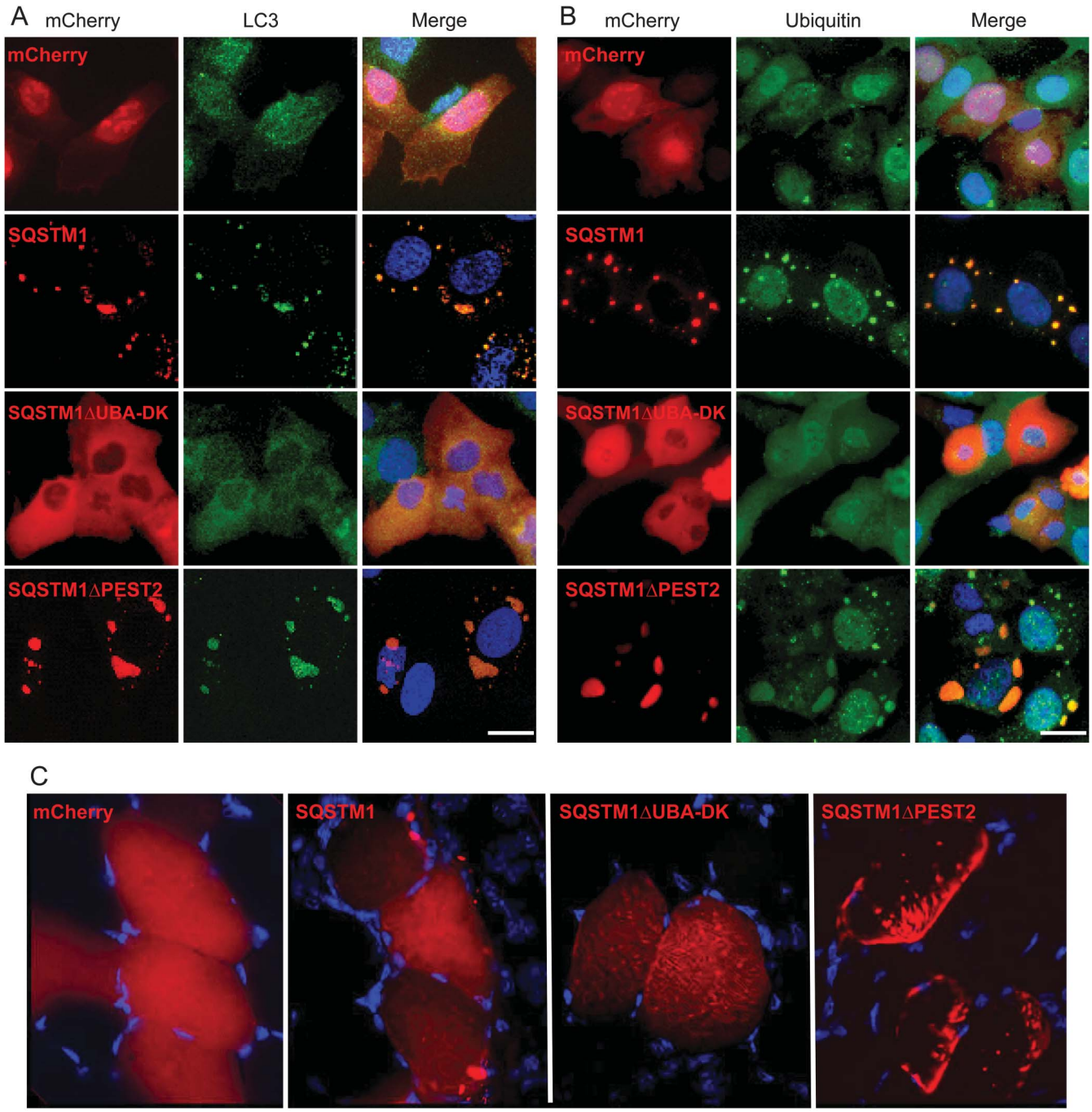

(A, B) U2OS cells were transiently transfected with plasmids expressing mCherry alone or mCherry fused to SQSTM1, SQSTM1ΔUBA-DK, or SQSTM1ΔPEST2 and immunostained with an antibody to (A) microtubule-associated protein 1A light chain-3 (LC3) or (B) ubiquitin. SQSTM1ΔUBA-DK is present diffusely throughout the cell and does not colocalize with LC3 or ubiquitin, whereas SQSTM1ΔPEST2 is present as large perinuclear inclusions that colocalize with both LC3 and ubiquitin. (C) Mouse tibialis anterior muscle was electroporated with plasmids expressing mCherry alone or mCherry fused to SQSTM1, SQSTM1ΔUBA-DK, or SQSTM1ΔPEST2, sectioned, and subjected to fluorescence microscopy. SQSTM1 is present both throughout the sarcoplasm and as larger inclusions. SQSTM1ΔUBA-DK does not form inclusions and is present on myofibrillar structures. In contrast, SQSTM1ΔPEST2 is present as large subsarcolemmal and sarcoplasmic inclusions.

throughout the cytoplasm and excluded from the nucleus. It did not localize to LC3 or ubiquitin. SQSTM1ΔPEST2 accumulated as large perinuclear inclusions that contained both LC3 and ubiquitin (figure 4, A and B). To see whether these patterns of SQSTM1 expression were found in muscle, we electroporated mouse TA muscle with similar expression constructs (figure 4C). As expected, mCherry was diffuse throughout myofibers. Overexpressed full-length SQSTM1 was present within the sarcoplasm and also as subsarcolemmal inclusions often adjacent to myonuclei. SQSTM1ΔUBA-DK

was present throughout the sarcoplasm and associated with myofibrillar structures. In contrast, SQSTM1ΔPEST2 was found only as large subsarcolemmal and sarcoplasmic inclusions.

DISCUSSION We expand the genetic etiology of AD distal myopathies with RVs to include *SQSTM1*. In addition, we expand the phenotypes associated with *SQSTM1* mutations to include myopathy. AD-inherited mutations in *SQSTM1* are associated with hereditary and sporadic forms of PDB, ALS, and FTD.[7,11,14] The identification of *SQSTM1* mutations in sporadic disease is likely due to its reduced penetrance.[7,15] Our report identified a c.1165+1 G>A transition in *SQSTM1* that was initially identified in an Australian family with PDB[11] and later identified in a French family with PDB.[12] More recently, a 75-year-old French woman with sporadic ALS manifesting as progressive distal lower limb weakness and PDB was found to have a c.1165+1 G>A transition in *SQSTM1*.[13] Neuropathologic assessment found TDP-43 and perinuclear SQSTM1 inclusions within the spinal cord and frontal cortex.[13] TDP-43 and SQSTM1 inclusions are a pathologic feature seen in myopathies with RVs[6,16] and were similarly found in the skeletal muscle of our patient carrying a *SQSTM1* mutation (figure 2, E and F). Notably, the patients described in this study did not have evidence of PDB, ALS, or FTD, suggesting that myopathy can occur in isolation with c.1165+1 G>A *SQSTM1* variant.

SQSTM1 is an adaptor that associates with ubiquitinated proteins and LC3 via its ubiquitin-associated (UBA) domain and LC3-interacting region to facilitate autophagic degradation.[17] SQSTM1 oligomerizes and also associates with another ubiquitin adaptor, neighbor of BRCA1 gene 1 (Nbr1), via its N-terminal Phox/Bem1p domain.[18] Nbr1 and SQSTM1 may act independently or together in the autophagic degradation of proteins.[19] SQSTM1 also regulates the Nrf2 antioxidant response pathway[20] and nutrient-sensed mTORC1 activity.[21] In skeletal muscle, SQSTM1 has more specialized roles. SQSTM1 complexes with the muscle-specific E3 ligase MuRF2 and Nbr1 on the giant sarcomeric protein titin to coordinate protein turnover.[22] Recently, it has been suggested that SQSTM1 and MuRF2 are necessary for the autophagic recycling of nicotinic acetylcholine receptors in skeletal muscle.[23]

The c.1165+1 G>A transition in *SQSTM1* leads to the generation of 2 abnormal protein species, both of which could be pathogenic (figure 3E). One species, missing a C-terminal PEST domain, is p.G351_P388del (SQSTM1ΔPEST2). SQSTM1 has 2 PEST domains with undefined function. PEST sequences are suggested to modulate protein stability since they are found on short-lived proteins.[24] The other translated protein species is an SQSTM1 truncation mutation, p.Glu389delinsAspLysTer (SQSTM1ΔUBA-DK). This species lacks the UBA domain and fails to associate with ubiquitinated proteins.[25] Two previous studies suggested that the c.1165+1 G>A transition in *SQSTM1* generated only the SQSTM1ΔUBA-DK translation product, calling it SQSTM1-A390X.[11,12] A subsequent study evaluated the c.1165+1 G>A transition in *SQSTM1* from transcripts generated in the spinal cord of a patient with ALS and identified the *SQSTM1* r.1052_1165del transcript, suggesting that only SQSTM1ΔPEST2 is produced.[13] Our study found that both SQSTM1ΔUBA-DK and SQSTM1ΔPEST2 are transcribed and translated into proteins.

When these truncation mutations were expressed in cells and muscle, their localization was distinct from wild-type SQSTM1 and from each other. SQSTM1ΔUBA-DK was diffuse throughout the cell and on striations in mouse skeletal muscle, consistent with its reported localization to titin's kinase domain.[22] In contrast, SQSTM1ΔPEST2 generated large cytoplasmic and sarcoplasmic inclusions containing ubiquitin and LC3. This pattern of SQSTM1 localization in skeletal muscle was reminiscent of that seen in our patient's muscle (figure 2F).

Several other SQSTM1 truncation mutations have been reported in patients with familial PDB, including Leu394Ter and Glu396Ter.[26] These truncated species also lack the C-terminal UBA domain but are not generated by cryptic splicing, supporting the hypothesis that SQSTM1ΔUBA-DK is the pathogenic species. However, missense mutations within the PEST2 domain of SQSTM1 have also been reported in sporadic and familial disease.[7,27]

Similar to mutations in *VCP*, *HNRNPA2B1*, and *HNRNPA1*, mutations in *SQSTM1* can lead to several different disease phenotypes, including rimmed vacuolar myopathy, ALS, FTD, and PDB.[4,9] Why some patients develop PDB or ALS and others develop a myopathy is unclear, but it may be related to the presence of other inherited genetic modifiers. Indeed, it has been suggested that an *APOE* ε4 allele increases the penetrance of FTD in patients with *VCP* mutations.[28] Whether a similar genetic factor increases risk for myopathy remains to be determined.

The disparate phenotypes in muscle, brain, spinal cord, and bone are unified by the pathologic accumulation of ubiquitin and TDP-43.[6,9] In some cases, SQSTM1, VCP, HNRNPA2B1, and HNRNPA1 also accumulate along with ubiquitin and TDP-43 in affected tissues.[9] These diseases have been categorized together using the nomenclature "multisystem proteinopathy" (MSP), with mutations in *VCP* causing

MSP1, mutations in *HNRNPA2B1* causing MSP2, and mutations in *HNRNPA1* causing MSP3.[9] We have now demonstrated that *SQSTM1* can cause a rimmed vacuolar myopathy in addition to ALS, FTD, and PDB and could thus be considered a multisystem proteinopathy or MSP4.

AUTHOR CONTRIBUTIONS

Robert Bucelli: drafting/revising the manuscript, study concept or design, analysis or interpretation of data, acquisition of data. Khalid Arhzaouy: drafting/revising the manuscript, study concept or design, analysis or interpretation of data. Alan Pestronk: drafting/revising the manuscript, study concept or design, analysis or interpretation of data, contribution of vital reagents/tools/patients. Sara Pittman: analysis or interpretation of data, acquisition of data. Luisa Rojas: drafting/revising the manuscript, acquisition of data. Carolyn Sue: drafting/revising the manuscript, analysis or interpretation of data, acquisition of data, obtaining funding. Anni Evilä: drafting/revising the manuscript, analysis or interpretation of data, contribution of vital reagents/tools/patients, acquisition of data. Peter Hackman: drafting/revising the manuscript, analysis or interpretation of data. Bjarne Udd: drafting/revising the manuscript, study concept or design, analysis or interpretation of data, acquisition of data, study supervision, obtaining funding. Matthew Harms: study concept or design, analysis or interpretation of data, acquisition of data. Conrad Weihl: drafting/revising the manuscript, study concept or design, analysis or interpretation of data, acquisition of data, statistical analysis, study supervision, obtaining funding. All authors accept responsibility for conduct of research and will give final approval.

STUDY FUNDING

Funding included NIH AG031867 (C.C.W.), NIH AG042095 (C.C.W.), the Muscular Dystrophy Association (C.C.W.), the Myositis Association (C.C.W.), and the Hope Center for Neurological Disorders (C.C.W. and M.B.H.).

DISCLOSURE

R. Bucelli and K. Arhzaouy report no disclosures relevant to the manuscript. A. Pestronk holds patents and receives royalties for TS-HDS antibody 7,175,989, issued 2007; GALOP antibody 6,121,004, issued 2000; GM1 ganglioside antibody 6,077,681, issued 2000; and Sulfatide antibody 6,020,140, issued 1995; and received speaker honoraria from Athena, 2007–2009. S. Pittman, L. Rojas, C. Sue, A. Evilä, P. Hackman, and B. Udd report no disclosures relevant to the manuscript. M. Harms received honoraria from Genzyme for speaking on neuromuscular genetics. C. Weihl received research funds from Ultragenyx Pharmaceuticals, Novato, CA. Go to Neurology.org for full disclosures.

Received December 22, 2014. Accepted in final form March 9, 2015.

REFERENCES

1. Udd B. Distal myopathies—new genetic entities expand diagnostic challenge. Neuromuscul Disord 2012;22:5–12.
2. Clemen CS, Herrmann H, Strelkov SV, Schroder R. Desminopathies: pathology and mechanisms. Acta Neuropathol 2013;125:47–75.
3. Palmio J, Sandell S, Suominen T, et al. Distinct distal myopathy phenotype caused by VCP gene mutation in a Finnish family. Neuromuscul Disord 2011;21:551–555.
4. Watts GD, Wymer J, Kovach MJ, et al. Inclusion body myopathy associated with Paget disease of bone and frontotemporal dementia is caused by mutant valosin-containing protein. Nat Genet 2004;36:377–381.
5. Ju JS, Fuentealba RA, Miller SE, et al. Valosin-containing protein (VCP) is required for autophagy and is disrupted in VCP disease. J Cell Biol 2009;187:875–888.
6. Weihl CC, Temiz P, Miller SE, et al. TDP-43 accumulation in inclusion body myopathy muscle suggests a common pathogenic mechanism with frontotemporal dementia. J Neurol Neurosurg Psychiatry 2008;79:1186–1189.
7. Fecto F, Yan J, Vemula SP, et al. SQSTM1 mutations in familial and sporadic amyotrophic lateral sclerosis. Arch Neurol 2011;68:1440–1446.
8. Gitcho MA, Baloh RH, Chakraverty S, et al. TDP-43 A315T mutation in familial motor neuron disease. Ann Neurol 2008;63:535–538.
9. Kim HJ, Kim NC, Wang YD, et al. Mutations in prion-like domains in hnRNPA2B1 and hnRNPA1 cause multisystem proteinopathy and ALS. Nature 2013;495:467–473.
10. Temiz P, Weihl CC, Pestronk A. Inflammatory myopathies with mitochondrial pathology and protein aggregates. J Neurol Sci 2009;278:25–29.
11. Hocking LJ, Lucas GJ, Daroszewska A, et al. Domain-specific mutations in sequestosome 1 (SQSTM1) cause familial and sporadic Paget's disease. Hum Mol Genet 2002;11:2735–2739.
12. Collet C, Michou L, Audran M, et al. Paget's disease of bone in the French population: novel SQSTM1 mutations, functional analysis, and genotype-phenotype correlations. J Bone Miner Res 2007;22:310–317.
13. Teyssou E, Takeda T, Lebon V, et al. Mutations in SQSTM1 encoding p62 in amyotrophic lateral sclerosis: genetics and neuropathology. Acta Neuropathol 2013;125:511–522.
14. Le Ber I, Camuzat A, Guerreiro R, et al. SQSTM1 mutations in French patients with frontotemporal dementia or frontotemporal dementia with amyotrophic lateral sclerosis. JAMA Neurol 2013;70:1403–1410.
15. Bolland MJ, Tong PC, Naot D, et al. Delayed development of Paget's disease in offspring inheriting SQSTM1 mutations. J Bone Miner Res 2007;22:411–415.
16. Nogalska A, Terracciano C, D'Agostino C, King Engel W, Askanas V. p62/SQSTM1 is overexpressed and prominently accumulated in inclusions of sporadic inclusion-body myositis muscle fibers, and can help differentiating it from polymyositis and dermatomyositis. Acta Neuropathol 2009;118:407–413.
17. Bjorkoy G, Lamark T, Brech A, et al. p62/SQSTM1 forms protein aggregates degraded by autophagy and has a protective effect on huntingtin-induced cell death. J Cell Biol 2005;171:603–614.
18. Lamark T, Perander M, Outzen H, et al. Interaction codes within the family of mammalian Phox and Bem1p domain-containing proteins. J Biol Chem 2003;278:34568–34581.
19. Kirkin V, Lamark T, Sou YS, et al. A role for NBR1 in autophagosomal degradation of ubiquitinated substrates. Mol Cell 2009;33:505–516.
20. Komatsu M, Kurokawa H, Waguri S, et al. The selective autophagy substrate p62 activates the stress responsive transcription factor Nrf2 through inactivation of Keap1. Nat Cell Biol 2010;12:213–223.
21. Duran A, Amanchy R, Linares JF, et al. p62 is a key regulator of nutrient sensing in the mTORC1 pathway. Mol Cell 2011;44:134–146.
22. Lange S, Xiang F, Yakovenko A, et al. The kinase domain of titin controls muscle gene expression and protein turnover. Science 2005;308:1599–1603.

23. Khan MM, Strack S, Wild F, et al. Role of autophagy, SQSTM1, SH3GLB1, and TRIM63 in the turnover of nicotinic acetylcholine receptors. Autophagy 2014;10:123–136.
24. Rogers S, Wells R, Rechsteiner M. Amino acid sequences common to rapidly degraded proteins: the PEST hypothesis. Science 1986;234:364–368.
25. Cavey JR, Ralston SH, Hocking LJ, et al. Loss of ubiquitin-binding associated with Paget's disease of bone p62 (SQSTM1) mutations. J Bone Miner Res 2005;20:619–624.
26. Hocking LJ, Lucas GJ, Daroszewska A, et al. Novel UBA domain mutations of SQSTM1 in Paget's disease of bone: genotype phenotype correlation, functional analysis, and structural consequences. J Bone Miner Res 2004;19:1122–1127.
27. Rubino E, Rainero I, Chio A, et al. SQSTM1 mutations in frontotemporal lobar degeneration and amyotrophic lateral sclerosis. Neurology 2012;79:1556–1562.
28. Mehta SG, Watts GD, Adamson JL, et al. APOE is a potential modifier gene in an autosomal dominant form of frontotemporal dementia (IBMPFD). Genet Med 2007;9:9–13.